

**A FLEXIBLE BAYESIAN FRAMEWORK TO ESTIMATE AGE- AND  
CAUSE-SPECIFIC CHILD MORTALITY OVER TIME FROM SAMPLE  
REGISTRATION DATA<sup>\*</sup>**

BY AUSTIN E. SCHUMACHER<sup>†</sup>, TYLER H. MCCORMICK<sup>†</sup>, JON WAKEFIELD<sup>†</sup>, YUE CHU<sup>§</sup>, JAMIE PERIN<sup>‡</sup>, FRANCISCO VILLAVICENCIO<sup>‡</sup>, NOAH SIMON<sup>†</sup>, AND LI LIU<sup>‡</sup>

*University of Washington<sup>†</sup>, Johns Hopkins University<sup>‡</sup> and The Ohio State University<sup>§</sup>*

*A. E. Schumacher*

*Department of Biostatistics  
University of Washington  
Seattle, WA 98195  
aeschuma@uw.edu*

*T. H. McCormick*

*Departments of Statistics and Sociology  
University of Washington  
Seattle, WA 98195  
tylernc@uw.edu*

*J. Wakefield*

*Departments of Biostatistics and Statistics  
University of Washington  
Seattle, WA 98195  
jonno@uw.edu*

*Y. Chu*

*Department of Sociology  
The Ohio State University  
Columbus, OH 43210  
chu.282@osu.edu*

*J. Perin*

*Department of International Health  
Johns Hopkins Bloomberg School of Public Health  
Baltimore, MD 21205  
jperin@jhu.edu*

*F. Villavicencio*

*Department of International Health  
Johns Hopkins Bloomberg School of Public Health  
Baltimore, MD 21205  
jf.villav1@jhu.edu*

*N. Simon*

*Department of Biostatistics  
University of Washington  
Seattle, WA 98195  
nrsimon@uw.edu*

*L. Liu*

*Departments of Population, Family and Reproductive Health and International Health  
Johns Hopkins Bloomberg School of Public Health  
Baltimore, MD 21205  
lliu26@jhu.edu*

---

<sup>\*</sup>Supported in part by NICHD grant #1R21HD095451-01 and the Bill & Melinda Gates Foundation, Investment ID: OPP1172551

*Keywords and phrases:* Bayesian inference, sample registration system, child mortality, cause-specific mortality.

In order to implement disease-specific interventions in young age groups, policy makers in low- and middle-income countries require timely and accurate estimates of age- and cause-specific child mortality. High quality data is not available in settings where these interventions are most needed, but there is a push to create sample registration systems that collect detailed mortality information. Current methods that estimate mortality from this data employ multistage frameworks without rigorous statistical justification that separately estimate all-cause and cause-specific mortality and are not sufficiently adaptable to capture important features of the data. We propose a flexible Bayesian modeling framework to estimate age- and cause-specific child mortality from sample registration data. We provide a theoretical justification for the framework, explore its properties via simulation, and use it to estimate mortality trends using data from the Maternal and Child Health Surveillance System in China.

**1. Introduction.** The [United Nations Inter-agency Group for Child Mortality Estimation \(2020\)](#) estimated that 5.2 million children worldwide died before five years of age in 2019. The international community is increasing investment to develop and implement age-targeted, disease-specific interventions and policy ([Glass, Guttmacher and Black, 2012](#); [Aponte et al., 2009](#); [Penny et al., 2016](#); [O'Brien et al., 2009](#); [Keenan et al., 2018](#)) that require knowing the patterns of child deaths for multiple causes across age and time. The burden of child deaths is heaviest in low and middle-income countries (LMICs) that lack high quality vital registration (VR) systems to register all births and deaths, creating massive uncertainty. The global health community has been pushing for drastic improvements in child health, most notably with the Sustainable Development Goals (SDGs) from the [United Nations \(2015\)](#). SDG 3 contains age- and cause-specific targets for reducing mortality. Assessing progress toward these goals and identifying areas for improvement require accurate estimation of cause-specific child mortality.

High quality VR data is the gold-standard for cause-specific child mortality. In most LMICs, however, VR systems are inadequate ([AbouZahr et al., 2015a,b](#); [Mikkelsen et al., 2015](#); [Phillips et al., 2015](#)). Instead, age- and cause-specific mortality data come from sample registration systems (SRS) and national/subnational surveys. Household verbal autopsy (VA) surveys comprise the bulk of national cause-specific mortality data ([Soleman, Chandramohan and Shibuya, 2006](#)). However, these data lack continuous monitoring provided by SRS. India and China have led the way in implementing nationally representative SRS ([Mahapatra, 2010](#); [Yang et al., 2005](#); [Liu et al., 2016a](#)), and calls for more and higher quality data collection ([Bchir et al., 2006](#); [Boerma and Stansfield, 2007](#); [Jha, 2012](#)) have encouraged establishment of SRS in countries such as Indonesia ([Rao et al., 2010](#)) and Mozambique ([Nkengasong et al., 2020](#)). Empirical estimates from SRS are noisy (see Figure 1), so as SRS data become increasingly available, developing a relevant modeling framework is crucial to produce cause-specific child mortality estimates that provide timely and useful information.

Three main methods are used to estimate cause-specific child mortality that are applicable to SRS data. The first, described by [Liu et al. \(2016b\)](#), models cause-specific mortality fractions (CSMFs) with a multinomial logistic regression model and then multiplies these by all-cause mortality rates estimated in a separate Bayesian framework ([You et al., 2015](#); [Alkema and New, 2014](#)) to produce cause-specific mortality rates (CSMRs). The second, used in the Global Burden of Disease study and detailed in [Vos et al. \(2020\)](#), models either rates or probabilities of death separately for each cause with an ad hoc ensemble modeling technique and then combines these with all-cause mortality rates estimated separately using a complex regression model described in [Wang et al. \(2020\)](#). The third, described by [He et al. \(2017\)](#), calculates all-cause mortality rates from a single SRS in China using a 3-year moving

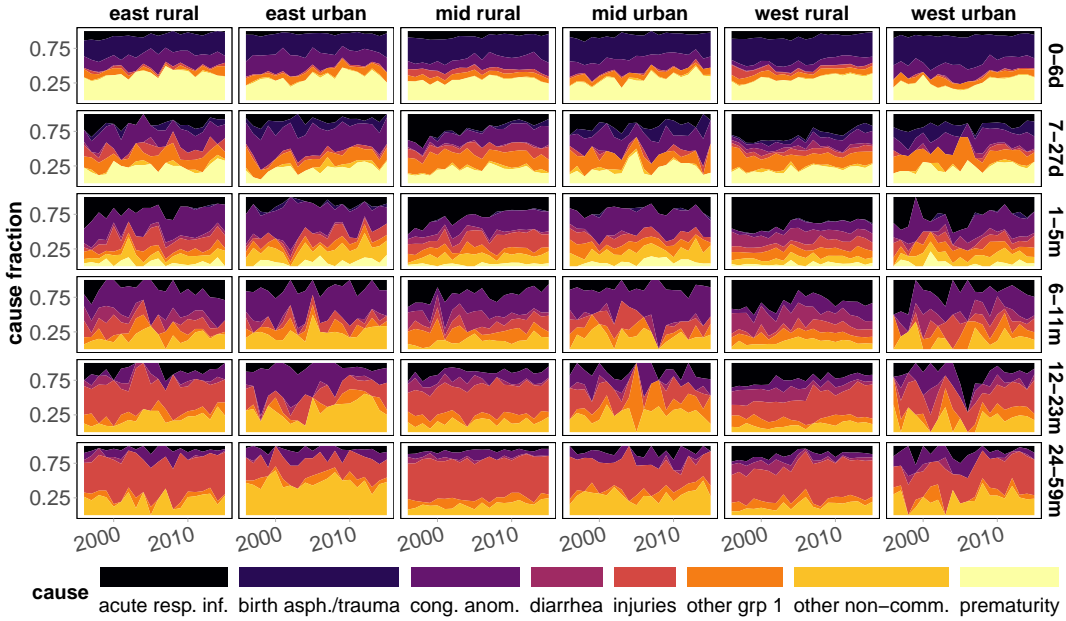


FIG 1. Empirical cause-specific mortality fractions over time by region and age group that were observed in the Maternal and Child Health Surveillance System in China.

average, proportionately scales them so they sum to the all-cause mortality rates estimated in You et al. (2015), and then multiplies these by estimated CSMFs at the age-region level that have been smoothed over time using a weighted seven-year moving average.

The primary issue with these methods is their use of multistage approaches that estimate all-cause and cause-specific mortality in separate, disconnected frameworks that do not “feed back” information and uncertainty between stages. A similar issue arises in sequential analysis (Bennett and Wakefield, 2001) which has been solved by building a full probability model (Plummer, 2015); the above multistage approaches fail to address this issue by leaving the models separate. Additionally, they reuse data in both stages, since data sources used for estimating cause-specific mortality are also used in the all-cause mortality models, violating assumed independence between data in the two stages and compromising uncertainty estimates.

Moreover, these multistage procedures cannot account for some features of the data that are important when modeling cause-specific mortality. For example, correlation between causes can arise when causes share a common underlying factor, such as measles and pertussis which are both influenced by vaccine access, and this factor is not included in the model. Vos et al. (2020) and He et al. (2017) model each cause separately, so no correlation parameters can be included. Liu et al. (2016b) do not model correlations, though the framework allows it. Beyond this, the multistage approach in He et al. (2017) facilitates improperly scaling to the national level using sampling probabilities without accounting for uncertainty.

Lastly, the approaches of Liu et al. (2016b) and He et al. (2017) produce estimates for broad 0–1 month and 1–59 month age groups that are not sufficient to capture variation in cause of death by age. The cause distribution for the ages within these broad age groups have much heterogeneity (Figure 1), but these approaches do not disaggregate further because the all-cause mortality estimates come from large global models that only estimate for broad ages, and a lack of smoothing across available variables prevents stable estimation for subgroups with limited data.

To address these issues, our paper brings together multiple strands of research to provide a modeling framework to estimate cause-specific child mortality rates from SRS data. We combine ideas from competing risks, loglinear modeling, and temporal smoothing to construct a framework for developing Bayesian models with efficient implementation. Our primary contribution is estimating all-cause and cause-specific child mortality in a unified process, rather than a misguided multistage approach, that provides more accurate inference and predictions. The flexibility of our framework allows different functional forms to be used as needed depending on context to model mortality at fine granularity by age, cause, region, time, or other strata. We demonstrate building a model using our framework and discuss issues to consider in a motivating example.

The remainder of this paper is structured as follows. Section 2 describes SRS data in general and details the data from our motivating example, the Maternal and Child Health Surveillance System (MCHSS) in China. Section 3 develops our proposed framework. Section 4 demonstrates improvements over multistage modeling approaches via simulation studies. Section 5 describes the use of our framework to develop and fit a model to the MCHSS data and compares our results to those from [He et al. \(2017\)](#). Section 6 provides a discussion and future steps.

**2. Data.** Here, we describe the data for our motivating example, the Maternal and Child Health Surveillance System (MCHSS) in China which is China's SRS devoted to maternal and child health. For a description of SRS data in general, see the supplementary material.

The MCHSS has a multistage, stratified, clustered sampling design that is regarded to be representative of the six region-residency strata, henceforth referred to as regions: east urban, east rural, mid urban, mid rural, west urban, and west rural. All children under 5 years of age living in the surveillance sites and all live births of mothers who are either permanent residents of the sites or have lived in the sites for at least 1 year are included. Deaths were assigned a single underlying cause that was ascertained via verbal autopsy, death certificate, or last clinical diagnosis. Deaths were aggregated to the six regions, 20 years of surveillance (1996–2015), six age groups (0–6 days, 7–27 days, 1–5 months, 6–11 months, 12–23 months, and 24–59 months) and 16 cause groups, and then adjusted upwards using a 3 year moving average of under-reporting rates estimated from an annual quality control study. Due to small numbers of deaths, the 16 causes were aggregated into 8 mutually exclusive, collectively exhaustive groups: prematurity, birth asphyxia/trauma, congenital anomalies, other non-communicable, injuries, diarrhea, acute respiratory infections, and other communicable. For prematurity and birth asphyxia/trauma, we deleted as outliers 20 deaths which were in age groups older than 6 months due to implausibility and to prevent unstable estimation from small death counts.

Person-years at risk were not available at the granularity of these six age groups. Therefore, tabulated exposure times were estimated by standard demographic methods described in the supplementary material. Although estimating exposure time is less exact than using recorded person-years under surveillance, exposure times are estimated in many other mortality estimation contexts using demographic methods or by making assumptions, e.g. using mid-year population estimates from the [United Nations Population Division \(2019\)](#). Furthermore, corrections for sampling and underreporting are commonly performed prior to analyses of census, survey, VR, and SRS data along with many other demographic modeling contexts ([Wang et al., 2020](#); [Vos et al., 2020](#); [Liu et al., 2016b](#); [He et al., 2017](#); [Wheldon et al., 2013](#)). These and other data issues are discussed in Section 6. For further details on data collection and production of adjusted and aggregated birth and death counts, we refer to the detailed description in [He et al. \(2017\)](#). Figure 1 shows empirical CSMFs over time by region and age. We provide death counts, estimated person-years, and log mortality rates by region, age, cause, and time period in the supplementary material.

**3. Statistical framework.** SRS data arise from a competing risks failure process, as described in [Prentice et al. \(1978\)](#). We assume that each death occurs from a single cause, and the set of causes is mutually exclusive and collectively exhaustive. We will begin by describing the individual-level likelihood and then consider modeling data tabulated by age, time period, and strata. A full derivation is provided in the supplementary material.

Let  $i \in \{1, \dots, n\}$  index individuals and  $c \in \{1, \dots, C\}$  index causes of death. Define  $T$  as a continuous random variable representing survival time and  $J$  as a random variable representing cause of death. We will parameterize survival time by age, i.e. time from birth for each individual. Let  $\mathbf{z}$  be the value of a covariate vector that we assume is fixed for convenience, although this work extends to time-varying covariates in the natural way. We define the cause-specific hazard, which in our case is the mortality rate, as  $\lambda_c(t|\mathbf{z}) = \lim_{\Delta t \rightarrow 0} P(t \leq T < t + \Delta t, J = c | T \geq t, \mathbf{z}) / \Delta t$ .

Suppose we have data where  $t_i$  is the time of observation,  $c_i$  is the cause of death,  $\delta_i = 1$  if a death is observed and  $\delta_i = 0$  otherwise (censored), and  $\mathbf{z}_i$  is a vector of fixed covariates for subject  $i$ . Let  $d_{ic}$  indicate that individual  $i$  dies from cause  $c$ . Note that  $d_{ic'} = 0$  for all  $c' \neq c_i$ , and for any censored observations,  $d_{ic} = 0 \forall i, c$ . We rewrite the likelihood from [Prentice et al. \(1978\)](#), up to proportionality and with independent censoring, as

$$(3.1) \quad \mathcal{L} = \prod_{i=1}^n \prod_{c=1}^C \left[ \lambda_c(t_i; \mathbf{z}_i)^{d_{ic}} \exp \left( - \int_0^{t_i} \lambda_c(u; \mathbf{z}_i) du \right) \right].$$

Next, suppose we instead have data tabulated into age groups  $k = 1, \dots, K$  and additional strata  $h = 1, \dots, H$ . Using arguments from [Holford \(1976\)](#), [Holford \(1980\)](#), and [Laird and Olivier \(1981\)](#), we define  $K$  intervals with breakpoints  $0 = \tau_0 < \tau_1 < \dots < \tau_K$ . Define  $d_{ihkc} = 1$  if individual  $i$  dies of cause  $c$  in age group  $k$  and strata  $h$ , and define  $t_{ihk}$  as the total time that individual  $i$  is observed in age group  $k$  and strata  $h$ . Note  $d_{ic} = \sum_{k=1}^K \sum_{h=1}^H d_{ihkc}$  because a person dies in only one age group and strata, and  $t_i = \sum_{k=1}^K \sum_{h=1}^H t_{ihk}$ . Define the observed data as  $y_{hkc} = \sum_{i=1}^n d_{ihkc}$ , the number of deaths in age group  $k$  and strata  $h$  from cause  $c$ , and  $t_{hk} = \sum_{i=1}^n t_{ihk}$ , the total person-time observed in age group  $k$  and strata  $h$ .

We will assume that cause-specific hazards are constant within each age-strata tabulation group, and for simplicity, we will assume no covariates. Thus,  $\lambda_c(t_i; \mathbf{z}_i) = \lambda_{hkc}$  for individual  $i$  in strata  $h$  with  $t_i \in [\tau_{k-1}, \tau_k]$ . However,  $\lambda_c(t; \mathbf{z})$  can depend on covariates and the following derivation extends naturally. The tabulated likelihood is found to be

$$(3.2) \quad \mathcal{L} = \prod_{h=1}^H \prod_{k=1}^K \prod_{c=1}^C [\lambda_{hkc}^{y_{hkc}} \exp(-\lambda_{hkc} t_{hk})].$$

This likelihood is identical to the kernel of the likelihood that would arise if  $y_{hkc} | \lambda_{hkc}, t_{hk} \sim \text{Poisson}(\lambda_{hkc} t_{hk})$ . Therefore, we can make likelihood-based inference using separate Poisson distributions for each cause and age group. This argument extends to any additional strata tabulations as well.

The multiple-Poisson likelihood in (3.2) is equivalent to a model in which the all-cause death counts and person-years have a Poisson distribution and the cause-specific counts conditional on the total death counts have a multinomial distribution. This equivalency of likelihoods is detailed in [Lee, Green and Ryan \(2017\)](#) and is commonly exploited in modeling multinomial count data. This gives rise to a specific multistage modeling specification: estimate all-cause mortality rates using a Poisson distribution and estimate CSMFs conditional on the all-cause death counts using a multinomial distribution. However, none of the multistage modeling approaches detailed in Section 1 specify this consistent two-stage likelihood.

Statistical modeling based on our framework provides the flexibility to choose a model for the CSMRs that is driven by the study-specific context. It is natural to work with loglinear hazard models due to the constraint that mortality rates must be positive. Then, given a vector of parameters  $\boldsymbol{\eta}$ , we can define a model as  $\log(\lambda_{hkc}) = f_{hkc}(\boldsymbol{\eta})$ . Using our proposed modeling framework, one can specify functional forms that contain fixed and random effects (Breslow and Clayton, 1993), use copula functions (Smith and Khaled, 2012), or any number of other methods. This flexibility is critical to account for the main drivers of mortality, but it also begets the need for careful model validation and comparison. We will discuss choosing a functional form, checking model adequacy, and comparing models when we engage with the MCHSS data in Section 5.

**4. Simulations.** This section compares models fit using our framework, which we call unified models, to models fit with a multistage framework that estimate CSMFs by combining separate cause-specific models. We fit models in this section with the INLA package for fast estimation using integrated nested Laplace approximation (Rue, Martino and Chopin, 2009) in the R statistical computing environment (R Core Team, 2013). Models use the default prior distributions in INLA. Full descriptions of each simulation are provided in the supplementary material. Replication code is available at <http://www.github.com/aeschuma/SRS-child-mortality>.

We do not compare methods with a multinomial model for CSMFs, such as Liu et al. (2016b), because our simulations model all-cause mortality rates with a Poisson distribution. This, in conjunction with a multinomial model for CSMFs conditional on the total death counts, leads to an equivalent likelihood to Equation 3.2 (Lee, Green and Ryan, 2017), show via simulation in the supplementary material. However, Liu et al. (2016b) do not use this consistent likelihood—rather, all-cause mortality estimates do not come from a Poisson model (Alkema and New, 2014), so consistency is not guaranteed.

**4.1. Scenario 1: Extra-Poisson Variability.** Let  $h \in \{1, \dots, H = 720\}$  index strata with 6 age groups, 6 regions, and 20 years, and let  $c \in \{1, \dots, C\}$  index cause. Define  $N_h$  as the total exposure time and  $y_{hc}$  as the death counts from cause  $c$  in strata  $h$ . Define  $\lambda_{hc}$  as the CSMRs,  $y_{h+} = \sum_c y_{hc}$  as the all-cause death counts and  $\lambda_{h+} = \sum_c \lambda_{hc}$  as the all-cause mortality rates.

For  $C = 8$  causes, we generate  $y_{hc}|\lambda_{hc} \sim \text{Poisson}(N_h\lambda_{hc})$ , with  $\log(\lambda_{hc}) = \alpha + \sum_{c'=2}^C \beta_{c'} \mathbb{1}_{[c'=c]} + \epsilon_{hc}$  and  $\epsilon_{hc}|\sigma_\epsilon^2 \sim \text{N}(0, \sigma_\epsilon^2)$ . This exemplifies a scenario with different mortality for each cause and extra-Poisson variability. We set  $\alpha = -5$ ,  $\beta_c = 0.5$  for all  $c$ , which yields death counts in the same range as the MCHSS data with a similar overall mean mortality rate of 0.01, and  $\sigma_\epsilon^2 = 0.2$ , which is approximately equal to the level estimated from our model fit to the MCHSS data described in Section 5.

For the multistage model, we estimate all-cause mortality rates using a Poisson GLMM with an overall intercept and IID Normal random effects on strata such that  $y_{h+}|N_h, \lambda_{h+} \sim \text{Poisson}(N_h\lambda_{h+})$ , with  $\log(\lambda_{h+}) = \alpha + \gamma_h$  and  $\gamma_h|\sigma_\gamma^2 \sim \text{Normal}(0, \sigma_\gamma^2)$ . To estimate the CSMFs, we use separate Poisson generalized linear mixed models each with an overall intercept and independent and identically distributed Normal random effects on strata. For each cause, we have  $y_{hc}|N_h, \lambda_{hc} \sim \text{Poisson}(N_h\lambda_{hc})$ , with  $\log(\lambda_{hc}) = \alpha_c + \xi_{hc}$  and  $\xi_{hc} \sim \text{Normal}(0, \sigma_{\xi_c}^2)$ .

Taking samples  $s = 1, \dots, 1000$  from the posteriors, for each sample we calculate CSMFs as  $\hat{p}_{hc}^{(s)} = \hat{\lambda}_{hc}^{(s)} / \sum_c \hat{\lambda}_{hc}^{(s)}$ , all-cause mortality rates as  $\hat{\lambda}_{h+}^{(s)}$ , and combine these to calculate log CSMRs as  $\log(\hat{\lambda}_{hc}^{(s)}) = \log(\hat{\lambda}_{h+}^{(s)} \hat{p}_{hc}^{(s)})$ .

To compare with the multistage model, we fit a unified model correctly specifying the data generating mechanism and draw 1000 posterior samples for each log CSMR.

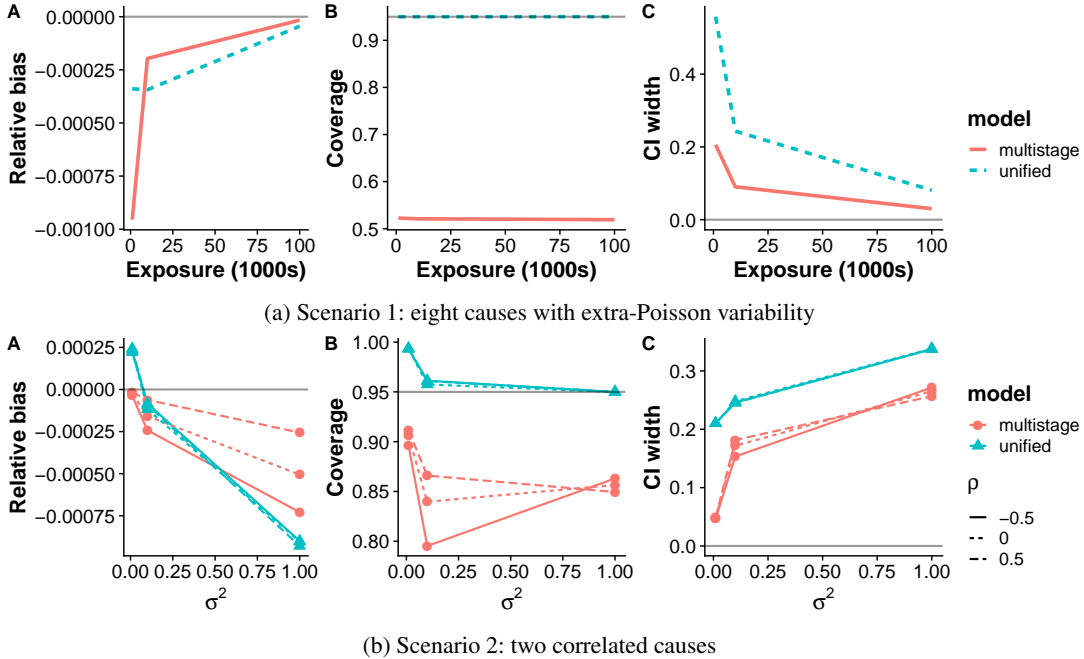


FIG 2. *Relative bias, coverage and width of 95% intervals for log mortality rates estimates from multistage and unified models. For (a), data were generated with IID Normal random effects for each observation and three possible exposure values. For (b), data were generated with bivariate IID Normal random effects for each region-age-year strata, defining the diagonal elements of the covariance matrix as  $\sigma^2$  and the off diagonal elements as  $\rho\sigma^2$ . Estimates are averaged over all observations and simulations per scenario.*

For both the multistage and unified models, we perform 100 simulations each for  $N_h \in \{1000, 10000, 100000\}$ . These are in the range of the 5th, 50th, and 95th percentiles of exposure time in the MCHSS data, which are 292, 8749, and 110974, respectively.

We compare the relative bias, coverage and width of posterior 95% intervals for log mortality rates as functions of exposure time in Figure 2. Neither approach is biased but the unified model has better coverage due to appropriately wider uncertainty intervals. The problem is likelihood misspecification, because the multistage model parameterizes the log of the sums of mortality rates as normally distributed, whereas in the generated data, the sum of the log mortality rates are normally distributed, which the unified model specifies correctly. This substantial undercoverage in the multistage model is derived analytically in the supplementary material. While we are imposing a normal distribution on the log cause-specific mortality rates in this example, which may not reflect the real world, we believe this parametric form is a relatively safe assumption since it corresponds to the canonical assumptions of exponential failure times in competing risks survival analysis.

**4.2. Scenario 2: correlated causes.** To show the benefits of our flexible framework for a contextually relevant situation in which a multistage approach fails, we simulate data for two causes with correlated CSMRs, representing causes with similar underlying drivers not captured in the data.

We use the same data generating mechanism as Scenario 1 with two changes. First, we include region and age as covariates with omitted reference groups and all associated coefficients equal to 0.5, in order to more closely resemble a situation where mortality depends on region and age. These again yield death counts and an overall mean mortality rate similar to the MCHSS data. Second, we specify  $\epsilon_h = (\epsilon_{h1}, \epsilon_{h2}) \sim N_2(\mathbf{0}, \Sigma)$  for the two causes. We set

the diagonal terms of  $\Sigma$  to be equal to  $\sigma^2$ , which controls overdispersion. The off-diagonal term is  $\sigma^2\rho$ , where  $\rho$  controls the correlation between causes. We set the exposure time to the median in the MCHSS.

We fit the same multistage model as the previous simulation, except both stages also include fixed effects for region and age, and compare it to a correctly specified unified model. We perform 100 simulations for each of nine scenarios:  $\sigma^2 \in \{0.01, 0.1, 1\}$  crossed with  $\rho \in \{-0.5, 0, 0.5\}$ . The values of  $\sigma^2$  span a range that are much smaller, similar to, and much larger than that estimated from the MCHSS data, and the values of  $\rho$  span a range that are consistent with residual correlations estimated from the MCHSS data in an exploratory analysis in the supplementary material.

Relative bias, coverage and width of 95% intervals for estimated log mortality rates as functions of  $\sigma^2$  for each value of  $\rho$  are shown in Figure 2. The bias in both models is negligible, although it increases slightly with higher overdispersion due to small-sample bias. We also see little direct impact of  $\rho$ . The coverage of the multistage model ranges between 80% and 90%, while the unified model has coverage near the nominal level with appropriately wider uncertainty intervals, although it displays overcoverage with small levels of overdispersion. This is not surprising because the elements of  $\Sigma$  are all nearly 0 in this case, so our model is estimating parameters for which there is very little information. This leads to overcoverage from additional uncertainty. The multistage model's undercoverage is again due to likelihood misspecification. In summary, the flexibility of our framework facilitates modeling aspects of the data, such as overdispersion and correlation, that a multistage model cannot, which leads to more accurate inference.

**5. Estimating mortality from SRS data.** This section uses our framework to develop a model to estimate child mortality from the MCHSS.

**5.1. Model description.** We index region by  $r \in \{1, \dots, R = 6\}$ , age group by  $a \in \{1, \dots, A = 6\}$ , year by  $t \in \{1, \dots, T = 20\}$ , and cause by  $c \in \{1, \dots, C = 8\}$ . Let  $N_{r,a,t}$  be person-years and  $y_{r,a,t,c}$  be death counts due to cause  $c$  in region  $r$ , age group  $a$ , and year  $t$ . To estimate cause-specific mortality rates by region and age over time, we specify the model as

$$(5.1) \quad \begin{aligned} y_{r,a,t,c} | N_{r,a,t}, \lambda_{r,a,t,c} &\sim \text{Poisson}(N_{r,a,t} \lambda_{r,a,t,c}) \\ \log(\lambda_{r,a,t,c}) &= \alpha + \beta_r^R + \beta_a^A + \beta_c^C + \\ &\quad \beta_{a,c}^{AC} + \beta_{r,c}^{RC} + \beta_{a,r}^{AR} + \\ &\quad \gamma_{r,a^*[a],c^*[c]}(t) + \epsilon_{r,a,t,c} \end{aligned}$$

In order to properly use a Poisson likelihood, we rounded deaths up to the nearest integer because the death counts in the MCHSS were fractional due to the underreporting adjustment described in Section 2.

In (5.1),  $\alpha$  is the overall intercept, and  $\beta_r^R$ ,  $\beta_a^A$ , and  $\beta_c^C$  are fixed effects for region, age, and cause, respectively. These are specified with omitted reference groups, i.e.  $\beta_1^R = \beta_1^A = \beta_1^C = 0$ . To capture first-order interactions, we include  $\beta_{a,c}^{AC}$ ,  $\beta_{r,c}^{RC}$ , and  $\beta_{a,r}^{AR}$  as fixed effects with omitted reference groups.

The parameter  $\gamma_{r,a^*[a],c^*[c]}(t)$  is a random effect on time with a second order random walk distribution that parameterizes the second differences in time as arising from a normal distribution, which we denote as  $\gamma_{r,a^*,c^*}(t) \sim \text{RW2}(\sigma_\gamma^2)$ . We include different random walks for various age-region-cause combinations and we share random walks among certain ages and

causes, hence indexing by  $a^*$  and  $c^*$ . We define  $a^*[a] = 1$  for observations in the 0–6 day age group ( $a = 1$ ) and  $a^*[a] = 2$  otherwise ( $a = 2, \dots, 6$ ). We define  $c^*[c] = 1$  for *diarrhea and other communicable diseases* ( $c = 1, 2$ ),  $c^*[c] = 2$  for *congenital anomalies and other non-communicable diseases* ( $c = 3, 4$ ), and  $c^*[c] = 3, \dots, 6$  for the remaining causes ( $c = 5, \dots, 8$ , respectively). This results in  $6$  (region)  $\times$   $2$  (age)  $\times$   $6$  (cause) =  $72$  random walks. All random walks share a variance parameter,  $\sigma_\gamma^2$  for parsimony and to reduce the number of estimated parameters to aid computation.

We specify  $\epsilon_{r,a,t,c} \stackrel{\text{iid}}{\sim} \text{Normal}(0, \sigma_\epsilon^2)$  with a penalized complexity prior on  $\sigma_\epsilon^2$  such that there is a 1% probability that  $\sigma_\epsilon > 5$ . We place proper but flat priors on the fixed effects. Prior choice is more important in more data sparse situations, but here estimating with stronger priors makes little difference.

To demonstrate adequacy of the model, we plotted the standardized residuals,  $(y_{r,a,t,c} - N_{r,a,t} \hat{\lambda}_{r,a,t,c}) / (N_{r,a,t} \hat{\lambda}_{r,a,t,c})^{1/2}$ , by all two- and three-way combinations of age, region, cause, and time. As a further exercise in model checking, we held out the final year of data, fit the model, predicted the log mortality rates, and then plotted these against the held out data.

We fit the model with the `INLA` package in R. All code used is available at <http://www.github.com/aeschuma/SRS-child-mortality>.

**5.2. Model development.** This section describes considerations for child mortality modeling and explains how our final model accounted for these.

**5.2.1. Cause.** The relative distribution of causes of death can vary immensely depending on the context of data collection (Clark, Setel and Li, 2019). In order for the competing risks framework to hold, we must have an exhaustive list of mutually exclusive causes with a sufficiently large number of deaths in each cause to provide stable estimation. For our model, we combined similar causes to achieve this. We used fixed effects for modeling due to the small number of causes and the strong differences in mortality.

Another consideration is that causes may be correlated due to covariates that were not collected but influence multiple causes of death, such as environmental factors. Modeling correlations may improve estimates, especially for time periods/regions/ages with little or no data. Unfortunately, estimating correlation parameters is difficult and requires large amounts of data. We performed a simulation study, presented in the supplementary material and further discussed in Section 6, in which we simulated two data sets with correlated CSMRs—one that was the same size as the MCHSS and one with 100 regions rather than six. The correlation parameters were well-estimated for the data with 100 regions but not for the MCHSS-sized data. Consequently, we did not model correlations in our final model.

**5.2.2. Time.** Prompt and accurate time trend estimates support policy enactment, intervention targeting, and resource allocation in an agile fashion (Friberg et al., 2010). In addition, they allow evaluation of performance toward child survival targets, such as the SDGs, and also serve as important quality indicators for global health statistics and their estimation (Walker, Bryce and Black, 2007). For data with a smaller time span than the MCHSS, modeling can be done via linear trends. As the number of available time points grows, then we recommend more flexible methods such as random walks or spline-based approaches.

For our model, we used a second order random walk to encourage the estimated mortality rates to vary smoothly in time. Mortality rates in the much larger population of China, which the  $\lambda_{r,a,t,c}$  parameters represent in our model, will have less yearly variability than exhibited in the MCHSS sample and we would expect them to vary smoothly. From this perspective, a random walk of the second order is preferred over the first order, which models the first

differences in time as being normally distributed, because a first order random walk allows for sharp year-to-year variation. Second order random walks are widely used in mortality modeling (Wakefield et al., 2019), as are spline cubic spline models (Alkema and New, 2014). A certain class of cubic splines are equivalent to second order random walks (Speckman and Sun, 2003). Another approach would be random effects with an autoregressive distribution (Chi and Reinsel, 1989).

**5.2.3. Age.** Mortality trends can vary drastically by age, which is important to model. For example, mortality reduction in neonatal ages has progressed less than in other ages (Liu et al., 2015). Age is commonly tabulated into groups. In the past, data for under-5 mortality has been disaggregated into the first year and the combined remaining four years; thankfully, recent data collection and estimation has favored further disaggregation into early- and late-neonatal, along with further breakdown of the 1–4 year period (Liu et al., 2016b; Vos et al., 2020). Finer age groups allow for more useful estimates to direct health interventions. Treating age as a categorical variable allows flexible, non-monotonic relationships, a modeling choice that is facilitated by the commonly-available tabulated form of SRS data.

With a small number of age groups, fixed intercepts are able to capture the main effects, which is what we used in our final model due to large differences in mortality among the tabulated groups in the MCHSS. Analyses using smaller scale survey data at the individual level can allow for age to be treated as continuous if desired, which allows the use of spline-based approaches or other flexible methods.

**5.2.4. Geography.** In the SDG era, health policy and program decision making are becoming decentralized with many decisions now happening at the district level. Subnational mortality estimates help adapt the development of health statistics to meet changing needs (Boerma, 2013). However, the level of disaggregation is limited by available geographic information. Coarsely aggregated data limits model choices to fixed effects. If detailed location information is available, many spatiotemporal methods with random effects can be adapted for use with our framework, for example the methods described in Wakefield et al. (2019). Data availability and the scale for reporting estimates should drive modeling choices. Some popular choices are the reparameterized Besag, York and Mollié model for areal data (Riebler et al., 2016) and the Gaussian Markov random field representation of the stochastic partial differential equations approach with a Matérn family for point-referenced data (Lindgren, Rue and Lindstrom, 2011).

The MCHSS data is aggregated into six policy-relevant regions that have similarities within the aggregated strata. As such, we modeled with fixed intercepts due to the small number of parameters needed and the limited benefit of borrowing information between regions.

**5.2.5. Interactions.** Interactions between cause, time, age, and geography are imperative because we expect differential effects for different combinations of these variables. The amount of data available restricts the number of interactions that can be fit, which means the context of the data analysis is crucial when choosing a model.

Due to the importance of time trends for global health policy and interventions, modeling different time trends for each age, region, and cause is paramount. For example, mortality rates from injuries are likely changing differently for infants compared to older children, and these may further be different in rural locations compared to urban locations. In our final model, we use different random walks in order to allow age-region-cause strata to have distinct trends. This accomplishes a similar goal as the model in He et al. (2017) without using ad-hoc weighted rolling averages. To aid computation, we share random walks among

certain ages and causes. The categories for sharing random walks were chosen via a data-driven exercise that accounted for the scientific context. We fit a suite of Poisson generalized linear models that contained interactions between time and all one-way, two-way, and three-way combinations of region, age, and cause, and then analyzed the residual plots for common patterns that were consistent with the context of child mortality in China. The 0–6 day age group had consistent patterns in the residuals that were different than the other ages, which is reasonable due to the biological uniqueness of this age group such as higher mortality and its dependence on birth-related interventions of health facilities. The causes that share random walks also had similar residual patterns which are reasonable because *diarrhea* and *other communicable diseases* are communicable, while *congenital anomalies* and *other non-communicable diseases* are non-communicable. This is fully detailed in the supplementary material.

We tested the feasibility of this by separately fitting random walk models for the data in each of the previously defined 72 age-region-cause combinations for random walks and comparing the estimated standard deviation parameters, which are presented in the supplementary material. The estimates ranged from 0.005 to 0.1, with the majority below 0.025. Sharing the variance parameter will shrink the rates of change in some of the time trends toward the average, but not drastically. For identifiability of second order random walks, we use sum-to-zero constraints along with an improper prior on the intercept  $\alpha$ , which ensures the resultant posterior is proper (Rue and Held, 2005). We use a penalized complexity prior (Simpson et al., 2017) such that there is a 1% probability that  $\sigma_\gamma > 1$ .

Other non-temporal interactions to consider include the different distributions of causes of death among age groups and regions, as well as different age effects among regions (WHO Collaborative Study Team on the Role of Breastfeeding on the Prevention of Infant Mortality, 2001; Walker et al., 2013; Abdullah et al., 2007; Snow et al., 1997). Accurate modeling of these allows interventions to be targeted to populations in most need. To determine how to model non-temporal interactions in the MCHSS data, initial data exploration using non-Bayesian GLMs showed that a generalized linear model with all three of these interactions had a substantially lower AIC than any model with only one of them included, and had only slightly higher AIC than a model that additionally included a three-way interaction. Because the model with a three-way interaction had approximately twice as many parameters, we chose to only include two-way interactions for parsimony.

**5.2.6. Overdispersion.** Overdispersion is common in child mortality data due to within-strata variability, such as from unobserved covariates. Furthermore, additional variability from measurement error, non-systematic errors from the data preprocessing steps, and cause misattribution must be accounted for. We include the  $\epsilon_{r,a,t,c}$  terms to account for these issues.

We treat  $\epsilon_{r,a,t,c}$  as an error term rather than true signal and do not use it to calculate the posterior distribution of our final estimates. While this parameter likely captures some true signal, we believe the relative strength of the signal is low because the data is a sample with quality issues, which will be discussed in Section 6. With more covariates and higher data quality, the magnitude of the noise component would decrease. Furthermore, by omitting  $\epsilon_{r,a,t,c}$ , our final estimates reflect the underlying smooth time trends. In contexts with more data, higher data quality, or where the goal is to estimate the true numbers of deaths in a population rather than underlying mortality rates, final CSMR estimates can include this parameter.

**5.2.7. Model validation and comparison.** Due to the flexibility of our framework and the many decisions that must be made when choosing how to model cause, time, age, geography, and their interactions, models must be checked for adequacy. We recommend plotting

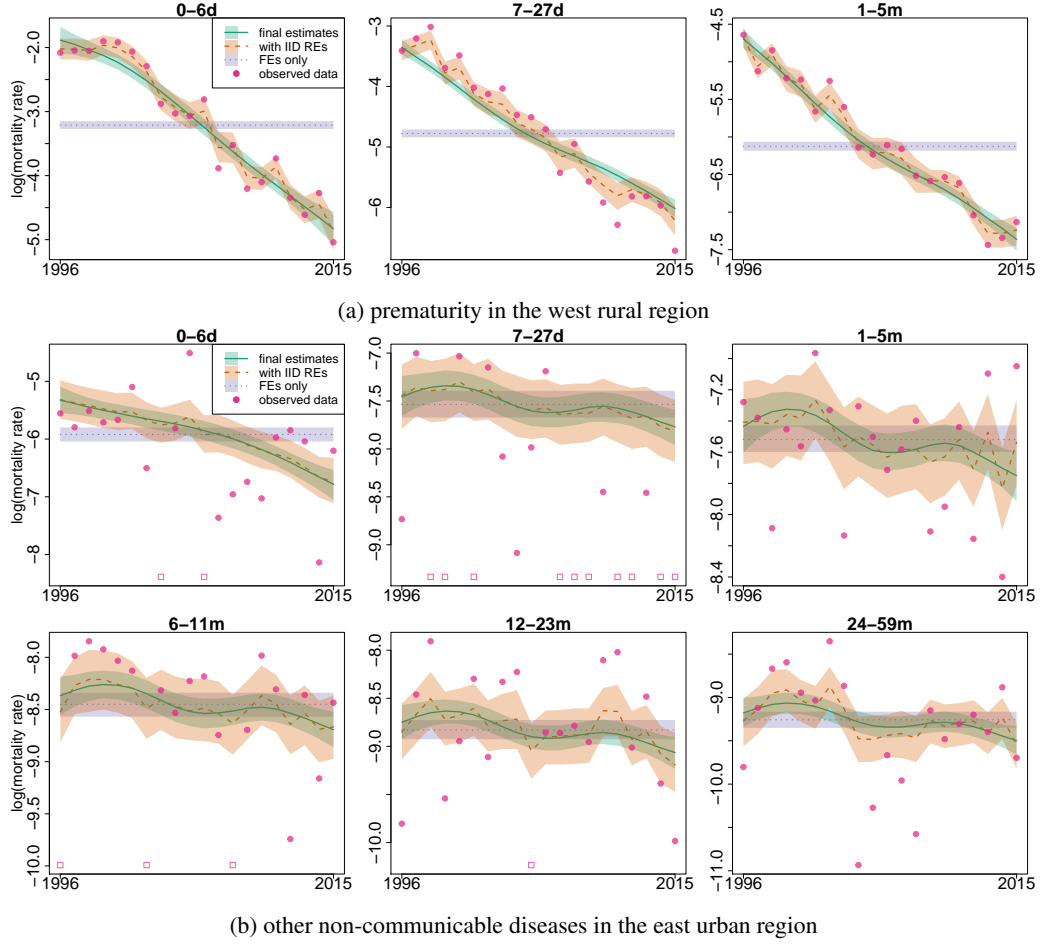


FIG 3. Selected results from the MCHSS data showing empirical data, estimated posterior medians, and posterior 80% intervals for log mortality rates. Combinations with no deaths are represented by an open square.

standardized residuals, i.e.  $(y_{r,a,t,c} - N_{r,a,t} \hat{\lambda}_{r,a,t,c}) / (N_{r,a,t} \hat{\lambda}_{r,a,t,c})^{1/2}$ , grouped by all combinations of each of the strata used in modeling (including two-way, three-way, and higher combinations if necessary). These plots should be examined for patterns that suggest inadequate model fit to the data. Furthermore, one can perform hold out experiments to evaluate predictive performance. For example, we held out the final year of observations in the MCHSS data, fit our model, and compared predictions to the observed data, since short-term predictions are relevant for policy decisions. Finally, we recommend comparing the performance of a suite of candidate models via traditional model comparison metrics such as the deviance information criteria (DIC), Watanabe-Akaike information criterion (WAIC), conditional predictive ordinates (CPO). For detailed discussion of model comparison, refer to [Gelman, Hwang and Vehtari \(2014\)](#) and [Held, Schrödle and Rue \(2010\)](#).

**5.3. Results.** Figure 3 shows estimated posterior medians and posterior 80% intervals for the log mortality rates over time in each age group for selected regions and causes. In order to show how the fixed effects component of the model contributes to these estimates, we include posterior medians and 80% intervals for the sum of the fixed effects only; to see the contribution of the random effect error terms,  $\epsilon_{r,a,t,c}$ , we also show the posterior medians and 80% intervals for the estimated log mortality rates with these added.

We first present estimates for prematurity in the west rural region, which represents the highest number of deaths in the data. Our model fits well, although the estimates are consistently higher than the observed data in the 7–27 day age group in later years, which is due to borrowing strength across other strata. This may indicate data errors, such as underreporting missed by the adjustment, or it may be due to shrinkage induced by the random walks. In comparison to preliminary models with random walks for each age-region combination only, the time trends for west rural prematurity were carried over to all causes and did not fit the data well. This is testament to the importance of including random walks by age-region-cause strata. Looking at a different cause and region, other non-communicable diseases in the east urban region, we see largely flatter time trends with wider uncertainty reflecting the smaller amount of data. In the random walk fitting exercise described in Section 5.2.5, this strata had a much lower estimated random walk variance parameter than the previous two strata presented, but all have acceptable fits here. Plots of all estimates from our final model are available in the supplementary material. Additionally in the supplementary material, we present estimated CSMFs over time for each age group and region to show differences in the distribution of causes by age and region over time. For example, the percentage of deaths due to congenital anomalies in the 1–5 and 6–11 month age groups is fairly constant in the east urban region but increasing in the mid rural region.

To show model adequacy, we present plots of standardized residuals by two- and three-way combinations of age, region, cause, and time, and plots of predicted vs. observed from a model with the final year held out. These show no gross misspecification and predictions with no systematic biases.

For model comparison, we fit a model with no interactions between fixed effects to assess the necessity of these interactions, and a model using first order autoregressive (AR1) processes rather than second order random walks to assess how we modeled temporal trends. We compared these to our final model via DIC, WAIC, and negative sum of the log CPO in the supplementary material. Not surprisingly, leaving out interactions caused a substantially poorer fit; the AR1 model was close but still inferior.

Since the method of [He et al. \(2017\)](#) also estimates cause-specific child mortality from the MCHSS data, we compare their results to our estimated CSMFs in the east rural region as an example in Figure 4. One primary benefit of our estimates is the more detailed age granularity. The approach in [He et al. \(2017\)](#) produced estimates for the 0–1 month and 1–59 month age groups. Any further disaggregation would presumably lead to unstable estimation as their model performs temporal smoothing from moving averages for each region-age-cause separately. In comparison, our method borrows strength across these dimensions which allows the further disaggregation into six age groups. Our estimates show substantial heterogeneity across the age groups that is masked by the large age bins in [He et al. \(2017\)](#). This figure also shows smoother temporal trends in our estimates, demonstrating less year-to-year variability which is what we expect for the population-level parameters in China that we are estimating from our sample. Furthermore, by proper smoothing methodology and variance estimation, we can make more definitive statements about smaller subgroups with uncertainty.

This comparison illustrates important conclusions that are missed by [He et al. \(2017\)](#). In the 0–1 month age group, [He et al. \(2017\)](#) estimate a large decline in the cause fraction for acute respiratory infections, resulting in a near-negligible percentage in 2015. However, our model shows that this cause is still meaningful in the 7–27 day age group. For intervention funding allocated in this region, our results indicate continued investment in acute respiratory infection prevention among children aged 7–27 whereas the results from [He et al. \(2017\)](#) do not. Another key takeaway is the comparatively larger portion of deaths due to injuries in the 24–59 month age group, along with smaller portions due to acute respiratory infections and congenital anomalies. This pattern could influence policies and resources to be enacted in a more targeted manner.

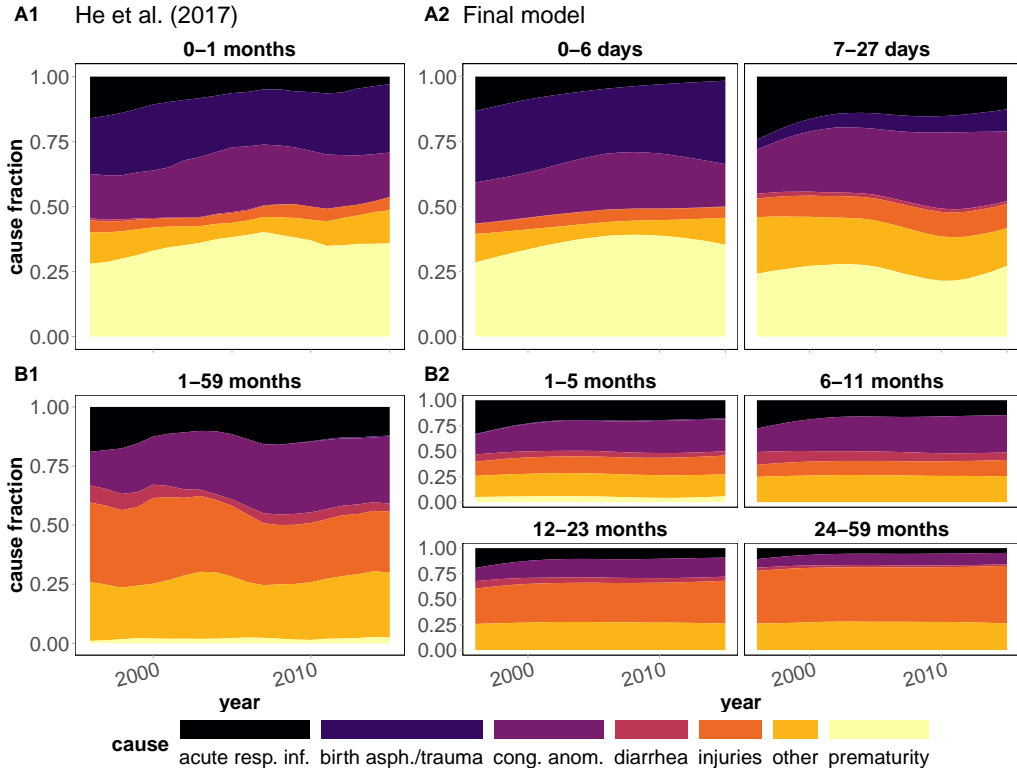


FIG 4. Comparisons of estimated CSMFs between our model and the model in [He et al. \(2017\)](#) in the east rural region. Panels A1 and B1 show cause fractions from [He et al. \(2017\)](#) for the 0–1 month and 1–59 month age groups, respectively, while panels A2 and B2 show the estimates from our model for the finer age groups as labeled that are within the broad age groups in A1 and B1.

**6. Discussion.** We have introduced a unified, flexible framework for estimating age- and cause-specific child mortality over time using tabulated death counts and exposure time from SRS data. This framework is based on an individual-level competing risks likelihood along with Bayesian smoothing priors. We have shown that it performs better than multistage modeling on simulated data with overdispersion and correlation, and we used the framework to develop a model for the MCHSS data from China.

Our framework improves upon current methodologies by simultaneously estimating all-cause and cause-specific mortality in a unified framework rather than using improper multistage models. We compared our model for the MCHSS data in China to the model in [He et al. \(2017\)](#). Our model improved estimation in four key ways: (1) [He et al. \(2017\)](#) improperly scales to national estimates as part of their multistage model, which is effectively unnecessary in our model because all-cause and cause-specific estimates are estimated simultaneously and consistently, which properly quantifies uncertainty; (2) we use a likelihood that is directly derived for tabulated death and exposure time data commonly reported from SRS which allows us to fully specify a flexible estimation model in a statistically well-grounded fashion; (3) we model temporal trends with second-order random walks rather than using ad hoc moving averages; and (4) we employ proper smoothing and variance estimation that allows stable estimates at finer subgroup granularity. Our estimates are smoother and tease out important heterogeneity in finer age groups that is missed in the results from [He et al. \(2017\)](#).

While we developed our framework to estimate child mortality from SRS data, it is applicable to other scenarios. We can use cause-specific child mortality data tabulated from

household surveys (as long as sampling probabilities are correctly accounted for), although modeling the individual data in this case may be preferred as discussed below. Additionally, high quality VR can be modeled with our framework, for which we recommend minimal smoothing due to near complete population coverage. Furthermore, by incorporating multiple types of data from multiple countries, our framework can be adapted for large scale estimation akin to [Liu et al. \(2016b\)](#) and [Vos et al. \(2020\)](#). This extension would be computationally expensive, however, necessitating developments to be explored in future research. Beyond child mortality, we can use our framework to develop models for estimating any rates with competing risks from data sources that provide tabulated counts and time-at-risk, or from which these values can be calculated. Some examples are cause-specific mortality for ages beyond 5 years, incidence of non-fatal diseases, and rates of traffic accidents by severity.

The high degree of flexibility in our framework allows complex trends to be estimated, but data availability should drive model choice. Simulation experiments with data generated similar to the true data can reveal what forms are estimable. As one example, we attempted an alternate specification for the MCHSS data that accounted for correlations between causes. We simulated data with the same size as the MCHSS that had correlated CSMRs and fit a correctly specified model. Recovery of the correlation parameters was poor and posterior distributions were wide. We then simulated data with 100 regions rather than six and fit a similar model. The correlation parameters were recovered well with narrow posterior distributions. Thus, we chose not to model correlation. A full description of this simulation exercise and its results are provided in the supplementary material.

Additionally, choosing prior distributions requires careful thought. We used diffuse priors for the fixed effects and penalized complexity priors for the variance parameters of the random walks and IID Normal random effects. The latter parameters are more sensitive to prior choice. We recommend penalized complexity priors due to the reasons outlined in [Simpson et al. \(2017\)](#) that allow for specifying context-relevant prior distributions. As sensitivity analyses for our model fit to MCHSS data, we fit one model with  $\text{Gamma}(5, 0.00005)$  priors on the precisions and one model with stronger  $\text{Normal}(0,5)$  priors on the fixed effects. No appreciable differences were found; the largest absolute difference in posterior median log mortality rates was 0.05.

We propose that the data context suggests the most important aspects of child mortality to model for the setting at hand. From this viewpoint, one could fit multiple candidate models and perform model assessment. The independent random effects are useful for this endeavor, for example plotting them against time to detect patterns. Cross validation is also useful and could include multiple levels depending on the context (e.g. leaving one observation out, leaving one region out, leaving one time period out). Different levels of cross validation explore aspects of the data for which different models may perform better ([Roberts et al., 2017](#)).

Finally, the MCHSS data provide an example of common problems to be addressed in SRS data. Underreporting adjustment and exposure time estimation are common data pre-processing steps. Beyond this, errors in cause attribution introduce substantial variability ([Desai et al., 2014](#); [Murray et al., 2014](#)). These issues naturally lead to using random effects in order to induce overdispersion which may accommodate this extra variability. If available, the unadjusted, unaggregated data would be used and the aggregation and completeness adjustments would be included as steps in the Bayesian modeling framework. Using individual-level data allows proper calculation of person-time, necessitating proper handling of the censoring for individual-level survival data. Individual-level data also require explicit incorporation of sampling probabilities either with design-based or model-based estimation ([Pfeffermann et al., 2013](#)). With individual-level VA data, probabilistic cause assignment could also be included, for example using the method in [McCormick et al. \(2016\)](#). Extending

our model in this manner would be necessary when using smaller scale surveillance data on individuals, e.g. data from COMSA Mozambique ([Nkengasong et al., 2020](#)), HDSS sites in the INDEPTH network ([Sankoh and Byass, 2012](#)), or HDSS sites in the ALPHA network ([Maher et al., 2010](#)). Future work could also expand this framework to include survey data, notably VA data, in a single model.

## SUPPLEMENTARY MATERIAL

### Supplementary material for “A flexible Bayesian framework to estimate age- and cause-specific child mortality over time from sample registration data”

([To be published](#)). The supplementary material provides an overview of SRS and associated data, an explanation of the method to calculate exposure time in the MCHSS, summary statistics for the MCHSS data, the full derivation of the proposed likelihood in Section 3, full descriptions of the simulations in Section 4 and additional analytical derivations of result, other simulations mentioned in Sections 4 and 6, descriptions and results of the model development exercises and analyses using the mortality estimates discussed in Section 5, graphs of all log mortality rate estimates from the MCHSS data from the final model, a graph of cause-specific mortality fractions over time by age and region, and plots demonstrating the fit and adequacy of the final model.

## REFERENCES

ABDULLAH, S., ADAZU, K., MASANJA, H., DIALLO, D., HODGSON, A., ILBOUDO-SANOGO, E., NHA-COLO, A., OWUSU-AGYEI, S., THOMPSON, R., SMITH, T. et al. (2007). Patterns of age-specific mortality in children in endemic areas of sub-Saharan Africa. *The American Journal of Tropical Medicine and Hygiene* **77** 99–105.

ABOUZAHR, C., DE SAVIGNY, D., MIKKELSEN, L., SETEL, P. W., LOZANO, R. and LOPEZ, A. D. (2015a). Towards universal civil registration and vital statistics systems: the time is now. *The Lancet* **386** 1407–1418.

ABOUZAHR, C., DE SAVIGNY, D., MIKKELSEN, L., SETEL, P. W., LOZANO, R., NICHOLS, E., NOTZON, F. and LOPEZ, A. D. (2015b). Civil registration and vital statistics: progress in the data revolution for counting and accountability. *The Lancet* **386** 1373–1385.

UNITED NATIONS INTER-AGENCY GROUP FOR CHILD MORTALITY ESTIMATION (2020). Levels & Trends in Child Mortality 2020 Technical Report, United Nations Children’s Fund.

ALKEMA, L. and NEW, J. R. (2014). Global estimation of child mortality using a Bayesian B-spline bias-reduction model. *The Annals of Applied Statistics* 2122–2149.

APONTE, J. J., SCHELLENBERG, D., EGAN, A., BRECKENRIDGE, A., CARNEIRO, I., CRITCHLEY, J., DAN-QUAH, I., DODOO, A., KOBBE, R., LELL, B. et al. (2009). Efficacy and safety of intermittent preventive treatment with sulfadoxine-pyrimethamine for malaria in African infants: a pooled analysis of six randomised, placebo-controlled trials. *The Lancet* **374** 1533–1542.

BCHIR, A., BHUTTA, Z., BINKA, F., BLACK, R., BRADSHAW, D., GARNETT, G., HAYASHI, K., JHA, P., PETO, R., SAWYER, C. et al. (2006). Better health statistics are possible. *The Lancet* **367** 190–193.

BENNETT, J. and WAKEFIELD, J. (2001). Errors-in-variables in joint population pharmacokinetic/pharmacodynamic modeling. *Biometrics* **57** 803–812.

BOERMA, J. T. (2013). Public health information needs in districts. *BMC Health Services Research* **13** S12.

BOERMA, J. T. and STANSFIELD, S. K. (2007). Health statistics now: are we making the right investments? *The Lancet* **369** 779–786.

BRESLOW, N. E. and CLAYTON, D. G. (1993). Approximate inference in generalized linear mixed models. *Journal of the American Statistical Association* **88** 9–25.

CHI, E. M. and REINSEL, G. C. (1989). Models for longitudinal data with random effects and AR (1) errors. *Journal of the American Statistical Association* **84** 452–459.

CLARK, S. J., SETEL, P. and LI, Z. (2019). Verbal Autopsy in Civil Registration and Vital Statistics: The Symptom-Cause Information Archive. *arXiv preprint arXiv:1910.00405*.

DESAI, N., ALEKSANDROWICZ, L., MIASNOKOF, P., LU, Y., LEITAO, J., BYASS, P., TOLLMAN, S., MEE, P., ALAM, D., RATHI, S. K. et al. (2014). Performance of four computer-coded verbal autopsy methods for cause of death assignment compared with physician coding on 24,000 deaths in low-and middle-income countries. *BMC Medicine* **12** 20.

UNITED NATIONS POPULATION DIVISION (2019). World Population Prospects Technical Report, Dept of International Economic and Social Affairs.

FRIBERG, I. K., KINNEY, M. V., LAWN, J. E., KERBER, K. J., ODUBANJO, M. O., BERGH, A.-M., WALKER, N., WEISSMAN, E., CHOPRA, M., BLACK, R. E. et al. (2010). Sub-Saharan Africa's mothers, newborns, and children: how many lives could be saved with targeted health interventions? *PLoS Medicine* **7** e1000295.

GELMAN, A., HWANG, J. and VEHTARI, A. (2014). Understanding predictive information criteria for Bayesian models. *Statistics and computing* **24** 997–1016.

GLASS, R. I., GUTTMACHER, A. E. and BLACK, R. E. (2012). Ending preventable child death in a generation. *Journal of the American Medical Association* **308** 141–142.

HE, C., LIU, L., CHU, Y., PERIN, J., DAI, L., LI, X., MIAO, L., KANG, L., LI, Q., SCHERPBIER, R. et al. (2017). National and subnational all-cause and cause-specific child mortality in China, 1996–2015: a systematic analysis with implications for the Sustainable Development Goals. *The Lancet Global Health* **5** e186–e197.

HELD, L., SCHRÖDLE, B. and RUE, H. (2010). Posterior and cross-validatory predictive checks: a comparison of MCMC and INLA. In *Statistical Modelling and Regression Structures* 91–110. Springer.

HOLFORD, T. R. (1976). Life tables with concomitant information. *Biometrics* 587–597.

HOLFORD, T. R. (1980). The analysis of rates and of survivorship using log-linear models. *Biometrics* 299–305.

JHA, P. (2012). Counting the dead is one of the world's best investments to reduce premature mortality. *Hypothesis* **10** e3.

KEENAN, J. D., BAILEY, R. L., WEST, S. K., ARZIKA, A. M., HART, J., WEAVER, J., KALUA, K., MRANGO, Z., RAY, K. J., COOK, C. et al. (2018). Azithromycin to reduce childhood mortality in sub-Saharan Africa. *New England Journal of Medicine* **378** 1583–1592.

LAIRD, N. and OLIVIER, D. (1981). Covariance analysis of censored survival data using log-linear analysis techniques. *Journal of the American Statistical Association* **76** 231–240.

LEE, J. Y., GREEN, P. J. and RYAN, L. M. (2017). On the "Poisson Trick" and its Extensions for Fitting Multinomial Regression Models. *arXiv preprint arXiv:1707.08538*.

LINDGREN, F., RUE, H. and LINDSTROM, J. (2011). An explicit link between Gaussian fields and Gaussian Markov random fields: the stochastic partial differential equation approach. *Journal of the Royal Statistical Society B* **73** 423–498.

LIU, L., HILL, K., OZA, S., HOGAN, D., CHU, Y., COUSENS, S., MATHERS, C., STANTON, C., LAWN, J. and BLACK, R. E. (2015). Levels and causes of mortality under age five years. *International Bank for Reconstruction and Development, World Bank. Reproductive, maternal, newborn, and child health: disease control priorities* **2** 71–83.

LIU, S., WU, X., LOPEZ, A. D., WANG, L., CAI, Y., PAGE, A., YIN, P., LIU, Y., LI, Y., LIU, J. et al. (2016a). An integrated national mortality surveillance system for death registration and mortality surveillance, China. *Bulletin of the World Health Organization* **94** 46–57.

LIU, L., OZA, S., HOGAN, D., CHU, Y., PERIN, J., ZHU, J., LAWN, J. E., COUSENS, S., MATHERS, C. and BLACK, R. E. (2016b). Global, regional, and national causes of under-5 mortality in 2000–15: an updated systematic analysis with implications for the Sustainable Development Goals. *The Lancet* **388** 3027–3035.

MAHAPATRA, P. (2010). An overview of the sample registration system in India. In *Prince Mahidol Award Conference & Global Health Information Forum* 27–30.

MAHER, D., BIRARO, S., HOSEGOOD, V., ISINGO, R., LUTALO, T., MUSHATI, P., NGWIRA, B., NYIRENDI, M., TODD, J., ZABA, B. et al. (2010). Translating global health research aims into action: the example of the ALPHA network. *Tropical Medicine & International Health* **15** 321–328.

MCCORMICK, T. H., LI, Z. R., CALVERT, C., CRAMPIN, A. C., KAHN, K. and CLARK, S. J. (2016). Probabilistic cause-of-death assignment using verbal autopsies. *Journal of the American Statistical Association* **111** 1036–1049.

MIKKELSEN, L., PHILLIPS, D. E., ABOUZahr, C., SETEL, P. W., DE SAVIGNY, D., LOZANO, R. and LOPEZ, A. D. (2015). A global assessment of civil registration and vital statistics systems: monitoring data quality and progress. *The Lancet* **386** 1395–1406.

MURRAY, C. J., LOZANO, R., FLAXMAN, A. D., SERINA, P., PHILLIPS, D., STEWART, A., JAMES, S. L., VAHDATPOUR, A., ATKINSON, C., FREEMAN, M. K. et al. (2014). Using verbal autopsy to measure causes of death: the comparative performance of existing methods. *BMC Medicine* **12** 5.

UNITED NATIONS (2015). Transforming our world: the 2030 Agenda for Sustainable Development. Resolution adopted by the General Assembly on 25 September 2015.

NKENGASONG, J., GUDO, E., MACICAME, I., MAUNZE, X., AMOUZOU, A., BANKE, K., DOWELL, S. and JANI, I. (2020). Improving birth and death data for African decision making. *The Lancet Global Health* **8** e35–e36.

O'BRIEN, K. L., WOLFSON, L. J., WATT, J. P., HENKLE, E., DELORIA-KNOLL, M., MCCALL, N., LEE, E., MULHOLLAND, K., LEVINE, O. S., CHERIAN, T. et al. (2009). Burden of disease caused by Streptococcus pneumoniae in children younger than 5 years: global estimates. *The Lancet* **374** 893–902.

WHO COLLABORATIVE STUDY TEAM ON THE ROLE OF BREASTFEEDING ON THE PREVENTION OF INFANT MORTALITY (2001). Effect of breastfeeding on infant and child mortality due to infectious diseases in less developed countries: a pooled analysis. *The Lancet* **355** 451–455.

PENNY, M. A., VERITY, R., BEVER, C. A., SAUBOIN, C., GALACTIONOVA, K., FLASCHE, S., WHITE, M. T., WENGER, E. A., VAN DE VELDE, N., PEMBERTON-ROSS, P. et al. (2016). Public health impact and cost-effectiveness of the RTS,S/AS01 malaria vaccine: a systematic comparison of predictions from four mathematical models. *The Lancet* **387** 367–375.

PFEFFERMANN, D. et al. (2013). New important developments in small area estimation. *Statistical Science* **28** 40–68.

PHILLIPS, D. E., ABOUZahr, C., LOPEZ, A. D., MIKKELSEN, L., DE SAVIGNY, D., LOZANO, R., WILMOTH, J. and SETEL, P. W. (2015). Are well functioning civil registration and vital statistics systems associated with better health outcomes? *The Lancet* **386** 1386–1394.

PLUMMER, M. (2015). Cuts in Bayesian graphical models. *Statistics and Computing* **25** 37–43.

PRENTICE, R. L., KALBFLEISCH, J. D., PETERSON JR, A. V., FLOURNOY, N., FAREWELL, V. T. and BRESLOW, N. E. (1978). The analysis of failure times in the presence of competing risks. *Biometrics* 541–554.

RAO, C., SOEMANTRI, S., DJAJA, S., ADAIR, T., WIRYAWAN, Y., PANGARIBUAN, L., IRIANTO, J., KOSEN, S., LOPEZ, A. D. et al. (2010). Mortality in Central Java: results from the indonesian mortality registration system strengthening project. *BMC Research Notes* **3** 325.

RIEBLER, A., SØRBYE, S. H., SIMPSON, D. and RUE, H. (2016). An intuitive Bayesian spatial model for disease mapping that accounts for scaling. *Statistical Methods in Medical Research* **25** 1145–1165.

ROBERTS, D. R., BAHN, V., CIUTI, S., BOYCE, M. S., ELITH, J., GUILLERA-ARROITA, G., HAUENSTEIN, S., LAHOZ-MONFORT, J. J., SCHRÖDER, B., THUILLER, W. et al. (2017). Cross-validation strategies for data with temporal, spatial, hierarchical, or phylogenetic structure. *Ecography* **40** 913–929.

RUE, H. and HELD, L. (2005). *Gaussian Markov random fields: theory and applications*. CRC Press.

RUE, H., MARTINO, S. and CHOPIN, N. (2009). Approximate Bayesian inference for latent Gaussian models by using integrated nested Laplace approximations. *Journal of the Royal Statistical Society B* **71** 319–392.

SANKOH, O. and BYASS, P. (2012). The INDEPTH Network: filling vital gaps in global epidemiology.

SIMPSON, D., RUE, H., RIEBLER, A., MARTINS, T. G., SØRBYE, S. H. et al. (2017). Penalising model component complexity: A principled, practical approach to constructing priors. *Statistical Science* **32** 1–28.

SMITH, M. S. and KHALED, M. A. (2012). Estimation of copula models with discrete margins via Bayesian data augmentation. *Journal of the American Statistical Association* **107** 290–303.

SNOW, R. W., OMUMBO, J. A., LOWE, B., MOLYNEUX, C. S., OBIERO, J.-O., PALMER, A., WEBER, M. W., PINDER, M., NAHLEN, B., OBONYO, C. et al. (1997). Relation between severe malaria morbidity in children and level of Plasmodium falciparum transmission in Africa. *The Lancet* **349** 1650–1654.

SOLEMAN, N., CHANDRAMOHAN, D. and SHIBUYA, K. (2006). Verbal autopsy: current practices and challenges. *Bulletin of the World Health Organization* **84** 239–245.

SPECKMAN, P. L. and SUN, D. (2003). Fully Bayesian spline smoothing and intrinsic autoregressive priors. *Biometrika* **90** 289–302.

R CORE TEAM (2013). R: A language and environment for statistical computing. *R Foundation for statistical computing*.

VOS, T., LIM, S. S., ABBAFATI, C., ABBAS, K. M., ABBASI, M., ABBASIFARD, M., ABBASI-KANGEVARI, M., ABBASTABAR, H., ABD-ALLAH, F., ABDELALIM, A. et al. (2020). Global burden of 369 diseases and injuries in 204 countries and territories, 1990–2019: a systematic analysis for the Global Burden of Disease Study 2019. *The Lancet* **396** 1204–1222.

WAKEFIELD, J., FUGLSTAD, G.-A., RIEBLER, A., GODWIN, J., WILSON, K. and CLARK, S. J. (2019). Estimating under-five mortality in space and time in a developing world context. *Statistical Methods in Medical Research* **28** 2614–2634.

WALKER, N., BRYCE, J. and BLACK, R. E. (2007). Interpreting health statistics for policymaking: the story behind the headlines. *The Lancet* **369** 956–963.

WALKER, C. L. F., RUDAN, I., LIU, L., NAIR, H., THEODORATOU, E., BHUTTA, Z. A., O'BRIEN, K. L., CAMPBELL, H. and BLACK, R. E. (2013). Global burden of childhood pneumonia and diarrhoea. *The Lancet* **381** 1405–1416.

WANG, H., ABBAS, K. M., ABBASIFARD, M., ABBASI-KANGEVARI, M., ABBASTABAR, H., ABD-ALLAH, F., ABDELALIM, A., ABOLHASSANI, H., ABREU, L. G., ABRIGO, M. R. et al. (2020). Global age-sex-specific fertility, mortality, healthy life expectancy (HALE), and population estimates in 204 countries and territories, 1950–2019: a comprehensive demographic analysis for the Global Burden of Disease Study 2019. *The Lancet* **396** 1160–1203.

WHELDON, M. C., Raftery, A. E., CLARK, S. J. and GERLAND, P. (2013). Reconstructing past populations with uncertainty from fragmentary data. *Journal of the American Statistical Association* **108** 96–110.

YANG, G., HU, J., RAO, K. Q., MA, J., RAO, C. and LOPEZ, A. D. (2005). Mortality registration and surveillance in China: history, current situation and challenges. *Population Health Metrics* **3** 3.

YOU, D., HUG, L., EJDEMYR, S., IDELE, P., HOGAN, D., MATHERS, C., GERLAND, P., NEW, J. R., ALKEMA, L. et al. (2015). Global, regional, and national levels and trends in under-5 mortality between 1990 and 2015, with scenario-based projections to 2030: a systematic analysis by the UN Inter-agency Group for Child Mortality Estimation. *The Lancet* **386** 2275–2286.